Proc. Natl. Acad. Sci. USA
Vol. 91, pp. 7237–7241, July 1994
Genetics

Structural analysis of chromosomal rearrangements associated with the developmental mutations *Ph*, W^{19H}, and *Rw* on mouse chromosome 5

(developmental genetics/physical maps/receptor tyrosine kinase)

DEBORAH L. NAGLE*, PATRICIA MARTIN-DELEON†, RICHARD B. HOUGH*, AND MAJA BUĆAN*‡

*Department of Psychiatry, University of Pennsylvania, Philadelphia, PA 19104; and †School of Life and Health Sciences, University of Delaware, Newark, DE 19716

Communicated by R. L. Brinster, March 24, 1994

ABSTRACT **We are studying the chromosomal structure of three developmental mutations, dominant spotting (*W*), patch (*Ph*), and rump white (*Rw*) on mouse chromosome 5. These mutations are clustered in a region containing three genes encoding tyrosine kinase receptors (*Kit*, *Pdgfra*, and *Flk1*). Using probes for these genes and for a closely linked locus, *D5Mit25*, we established a high-resolution physical map covering ≈2.8 Mb. The entire chromosomal segment mapped in this study is deleted in the W^{19H} mutation. The map indicates the position of the *Ph* deletion, which encompasses not more than 400 kb around and including the *Pdgfra* gene. The map also places the distal breakpoint of the *Rw* inversion to a limited chromosomal segment between *Kit* and *Pdgfra*. In light of the structure of the *Ph–W–Rw* region, we interpret the previously published complementation analyses as indicating that the pigmentation defect in *Rw*/+ heterozygotes could be due to the disruption of *Kit* and/or *Pdgfra* regulatory sequences, whereas the gene(s) responsible for the recessive lethality of *Rw/Rw* embryos is not closely linked to the *Ph* and *W* loci and maps proximally to the W^{19H} deletion. The structural analysis of chromosomal rearrangements associated with W^{19H}, *Ph*, and *Rw* combined with the high-resolution physical mapping points the way toward the definition of these mutations in molecular terms and isolation of homologous genes on human chromosome 4.**

Three mutations on mouse chromosome 5, dominant spotting (*W*), patch (*Ph*), and rump white (*Rw*), were historically described as a gene triplet on the basis of their close linkage and similar mutant phenotypes (1). Molecular analysis of these three loci has progressed rapidly due to the findings that *W* and *Ph* are associated with mutations and/or chromosomal rearrangements of genes encoding receptor tyrosine kinases (RTKs) (2). RTKs are known to have an important role in the regulation of growth and differentiation (3).

There are multiple alleles of *W*, which vary in their degree of severity and in their pleiotropic effects on melanogenesis, hematopoiesis, and germ cell development (4). Analysis of the protooncogene c-*kit* (a RTK) in several independently identified *W* alleles demonstrated that the *W* mutant phenotype is due to mutations that affect either the structure of the Kit receptor or the level and spatial distribution of *Kit* expression (5–10). More recently, it has been shown that the product of the *Sl* locus on mouse chromosome 10 encodes the ligand for the Kit receptor (reviewed in ref. 2).

The *Ph* mutation is associated with a dominant white spotting phenotype characterized by a depigmented belt around the abdomen (1, 11). *Ph/Ph* homozygotes die around midgestation and, prior to their death, embryos display several morphological abnormalities (e.g., small size, undifferentiated somites, abnormal heart, wavy neural tube) (11–13). The *Ph* locus encodes the platelet-derived growth factor receptor α subunit, *Pdgfra*, a member of the RTK gene family (14, 15). It is not known, however, whether the mutant phenotype of *Ph/Ph* embryos is due solely to the deletion of *Pdgfra* or to the deletion of an additional closely linked gene(s).

The W^{19H} allele is a deletional mutation spanning 2–7 centimorgans (cM), encompassing both the *Ph* and *W* loci, and a recessive lethal (*l*), which has yet to be defined at a molecular level (15–17). The hypopigmentation associated with the W^{19H} mutation in mice is strikingly similar to the observed depigmentation in humans with the piebald trait. This developmental defect is caused by a deletion of the homologous portion of human chromosome 4 containing the *Kit* and *Pdgfra* genes (18–20).

The *Rw* mutation is characterized by heterozygous spotting of the posterior trunk; the embryonic lethality of *Rw/Rw* mice occurs during midgestation as a result of unknown causes (1). Although a candidate gene for the *Rw* mutation has not been identified, it has been shown recently that this irradiation-induced mutation is associated with an inversion involving the proximal one-third of the chromosome. The distal breakpoint of the inversion has been mapped by *in situ* analysis to the chromosomal segment spanning 4 cM between the *Kit* and *D5Buc1* loci, while the proximal breakpoint maps centromeric to the engrailed 2 (*En2*) locus (21).

The cluster of RTKs (class III subfamily) located in the central portion of mouse chromosome 5 includes at least three members: *Kit*, *Pdgfra*, and *Flk1* (22–24). Previously, *Kit* and *Pdgfra* have been linked genetically and physically to one another (14, 15, 25). *Flk1*, an endothelial cell-specific RTK, has been genetically linked to the *Kit* locus (24).

In an attempt to determine the molecular basis of the *Ph*, *Rw*, and W^{19H} mutations and to assess the role of the cluster of RTKs on mouse chromosome 5 in development, we have established a high-resolution physical map covering 2.8 Mb of that region on the wild-type (C57BL/6J) chromosome. In addition, we have determined the approximate map position of the breakpoints of the *Ph* deletion and placed the distal breakpoint of the *Rw* inversion on the physical map. The map indicates close proximity (within 200 kb) of sequences disrupted by the *Ph* and *Rw* chromosomal anomalies. We have utilized the wealth of previously published genetic data on

The publication costs of this article were defrayed in part by page charge payment. This article must therefore be hereby marked "*advertisement*" in accordance with 18 U.S.C. §1734 solely to indicate this fact.

Abbreviations: RTK, receptor tyrosine kinase; cM, centimorgan(s); YAC, yeast artificial chromosome; PFGE, pulsed-field gel electrophoresis; FISH, fluorescence *in situ* hybridization; FITC, fluorescein isothiocyanate; PI, propidium iodide; DAPI, diaminophenylindole.

‡To whom reprint requests should be addressed at: Department of Psychiatry, University of Pennsylvania, 111A CRB, 422 Curie Boulevard, Philadelphia, PA 19104-6141.

Ph+/+*Rw* and *Rw*+/+W^{19H} compound heterozygotes to suggest that the embryonic lethality of *Rw*/*Rw* embryos is probably due to the disruption of a gene at the proximal breakpoint of this inversion, near the centromeric portion of mouse chromosome 5.

MATERIALS AND METHODS

Mice. Mouse inbred strains (C57BL/6J, C3H/HeJ, and *Mus spretus*) and mutations (W^{19H}, *Ph*) were obtained from The Jackson Laboratory. *Rw* mice were provided by Bruce Cattanach (Medical Research Council Radiobiology Unit, Harwell, U.K.). Mice used for deletion mapping were the F_1 progeny from the following crosses: W^{19H}/C57BL/6J × *M. spretus* and *Ph*/C57BL/6J × *M. spretus*.

DNA Probes. The DNA probes used in this study are a 0.6-kb *Hin*dIII fragment of the fetal liver kinase 1 gene (*Flk1*) (24); a 1.2-kb *Eco*RI/*Sph* I fragment of the c-*kit* protooncogene cDNA (*Kit*) (5′ portion of the gene) and a 0.9-kb *Hin*dIII fragment of *Kit* (3′ portion of the gene) (P. Dubreuil and A. Bernstein, personal communication); a 1.8-kb *Eco*RI/*Hin*dIII fragment of the platelet-derived growth factor receptor α cDNA (*Pdgfra*) (5′ portion) and a 2-kb *Eco*RI/*Hin*dIII fragment of the *Pdgfra* (3′ portion of the gene) (26); a 0.4-kb *Eco*RI/*Hin*cII fragment of an anonymous brain cDNA (*D5Mnl25*) (17); a 0.5-kb *Eco*RI/*Hin*dIII fragment (*D5Buc2*) corresponding to the right end and a 0.4-kb *Eco*RI/*Hae* III fragment (*D5Buc3*) corresponding to the left end of a *Pdgfra* yeast artificial chromosome (YAC) (ICRFy902G08127) (this paper); and a 0.6-kb *Pst* I fragment of the random DNA probe (*D5Buc1*) (ref. 21; J. DeLoia, M.B., and D. Solter, unpublished data).

Analysis by Pulsed-Field Gel Electrophoresis (PFGE). Methods for PFGE, including DNA preparation in agarose blocks and restriction analysis, have been described (27). DNA separated by PFGE was transferred to Hybond N^+ (Amersham) membrane by capillary blotting in denaturation buffer (28), UV crosslinked (autocrosslink set up on Stratalinker, Stratagene), and hybridized as described (27).

Isolation of YAC Clone. A YAC clone for *Pdgfra* was obtained by screening high-density robot spotted filters containing a mouse (C3H/He) YAC library (29), generously provided by H. Lehrach (Imperial Cancer Research Fund, London). After a rescreen, DNA from a positive clone was isolated by using published protocols (30). YAC ends were isolated by the inverse PCR procedure (31).

Fluorescence *in Situ* Hybridization (FISH) Analysis. Mitotic spreads were prepared from spleen lymphocytes of *Rw* heterozygotes by using a modification of the procedure described by Sawyer *et al.* (32). YAC DNA used for *in situ* hybridization was isolated by separating yeast DNA by PFGE. Purified YAC DNA was biotin-labeled by random priming. The hybridization probe was prepared by mixing 400 ng of biotinylated YAC DNA with 6.25 μg of mouse genomic DNA and 12.5 μg of salmon sperm DNA in hybridization buffer (Hybrisol VII; Oncor). It was applied to denatured chromosomal DNA on slides, which were incubated for 16 hr at 37°C. Slides were washed five times for 5 min each at 42°C in 50% formamide/2× standard saline citrate (SSC) with the last wash in 0.1× SSC. Detection and amplification of the labeled probe were performed using fluorescein isothiocyanate (FITC)-avidin and anti-avidin (Oncor detection kit) and slides were stained in 1.5 μg of propidium iodide (PI) per ml, 1.5 μg of diaminophenylindole (DAPI) per ml, and 1 mg of *p*-phenylenediamine per ml. A triple bandpass filter for DAPI/FITC/rhodamine was used for chromosome identification and a dual-wavelength filter cube (FITC and rhodamine) was used for signal visualization.

RESULTS

Physical Map. In our attempt to analyze the chromosomal structure and rearrangements associated with the *Ph*, W^{19H}, and *Rw* mutations, we made use of the available molecular probes to establish a long-range restriction map of the corresponding chromosomal region on the wild-type chromosome. The gene probes, *Flk1*, *Kit*, and *Pdgfra*, and an anonymous cDNA, *D5Mnl25*, the first molecular marker mapped within the W^{19H} deletion (17), were used in PFGE analysis of C57BL/6J DNA. In addition, we used end clones (*D5Buc2* and *D5Buc3*) of a *Pdgfra*-containing YAC. All molecular probes were sequentially hybridized to filters containing splenocyte DNA digested with *Bss*HII, *Mlu* I, *Not* I, and combinations of these enzymes. Analysis of the hybridization patterns and fragment sizes (Table 1) allowed the construction of a long-range restriction map spanning 2.8 Mb (Fig. 1*A*). The established order of loci is *D5Mnl25*–*D5Buc2*–*Pdgfra*–*Kit*–*Flk1*. Although the map spans 2.8 Mb, the three homologous RTK genes, *Pdgfra*–*Kit*–*Flk1*, map within 1 Mb.

Deletion Mapping of *Ph* and W^{19H} Chromosomes. Two mutations included in this study, *Ph* and W^{19H}, have been associated with deletions of genetic material (5, 14–17). To determine the positions of the deletion breakpoints on the physical map, we used the same molecular probes included in the PFGE analysis and an additional locus, *D5Buc1*, located 4 cM proximal to *Kit* (21). These probes were analyzed by Southern blot hybridization in DNA isolated from F_1 progeny of the following interspecific crosses: *Ph*/C57BL/6J × *M. spretus* and W^{19H}/C57BL/6J × *M. spretus*. Since the tested molecular probes detected restriction fragment length variants between *M. spretus* and *Mus musculus* (carrying the *Ph* and W^{19H} deletions), it was possible to distinguish the two parental chromosomes and determine whether any of these sequences are deleted on the *Ph* and/or W^{19H} chromosome (data not shown). The results of deletion mapping are summarized in Fig. 1*B*. The *D5Buc1* locus maps outside the W^{19H} and *Ph* deletions; *D5Mnl25*, and *Kit*, and *Flk1* are deleted in W^{19H} but not on the *Ph* chromosome, whereas *Pdgfra* is deleted on the W^{19H} and *Ph* chromosomes. One end clone, *D5Buc3*, maps within the *Ph* deletion, while the other clone, *D5Buc2*, maps outside the deletion.

FISH Mapping of *Pdgfra* on the *Rw*/C57BL/6J Chromosome. Previous work has demonstrated that the distal breakpoint of the inversion associated with the *Rw* mutation maps to a 4-cM region between *D5Buc1*, a locus within the inversion, and *Kit*, which is located outside the inversion (21). To define the location of the distal inversion breakpoint we used

Table 1. Summary of fragment sizes

Restriction enzyme	*Flk1*	*Kit*	*Pdgfra, D5Buc3*	*D5Buc2*	*D5Mnl25*
Not I	600	600	510	900	560
Mlu I	540	550, (680)	550, (680)	1500	1500
*Bss*HII	260, (570)	360, (570)	440	(260), 550	240, 450
Not I + *Mlu* I	370	150, 260	435	350, 900	550
Not I + *Bss*HII	260, (300)	360, (570)	440	(260), 550	240, (400), 450
Mlu I + *Bss*HII	260, (300)	150, 260	440	(260), 550	240, (400), 450

Partially cut bands are indicated in parentheses.

FISH analysis of *Rw*/C57BL/6J metaphase spreads and the *Pdgfra* YAC as a probe. Fig. 2 shows that the position of the signal for the *Pdgfra* gene differs on the two homologues of chromosome 5. On one chromosome, the hybridization signal is confined to the central portion of the chromosome, corresponding to the location on the wild-type chromosome (21), whereas on the other chromosome it is located near the centromeric heterochromatin. Since it has been previously shown by FISH analysis that *Kit* maps to the same location on both homologues (21), we can strongly argue that the breakpoint of the *Rw* inversion must be located between *Kit* and *Pdgfra*.

PFGE Analysis of *Ph*/C57BL/6J and *Rw*/C57BL/6J Chromosomes. The physical mapping data demonstrate that the *Kit* and *Pdgfra* genes are located on a *Mlu* I DNA fragment of 550 kb and that they share an additional partially digested *Mlu* I fragment of 680 kb (Table 1; Fig. 1*A*; ref. 15). Stephenson *et al.* (14) demonstrated that *Pdgfra* is deleted in the *Ph* mutation and that *Kit* genomic sequences are not disrupted in *Ph*, thus defining the position of the distal breakpoint of the *Ph* deletion as lying between *Pdgfra* and *Kit*. Here, we demonstrate by FISH analysis that the same chromosomal region is associated with the distal breakpoint of the *Rw* inversion (Fig. 2; ref. 21). Conventional Southern blot analysis of genomic sequences surrounding the *Kit* gene in DNA from *Ph*/C57BL/6J and *Rw*/C57BL/6J indicated no alterations (data not shown), nor were there any alterations of *Rw*/C57BL/6J DNA detected with the *Pdgfra* probe. However, chromosomal rearrangements were detected by PFGE analysis of large fragments containing the two genes.

We mapped the proximal breakpoint of the *Ph* deletion by PFGE of heterozygous (*Ph*/C57BL/6J) DNA. Molecular probes from the *W–Ph–Rw* region were hybridized to C57BL/6J and *Ph*/C57BL/6J DNA digested with *Bss*HII, *Mlu* I, *Not* I, and combinations of these enzymes. The YAC end, *D5Buc2*, shown to map outside the *Ph* deletion by deletion mapping (Fig. 1*B*), detects all C57BL/6J-specific fragments and additional, larger fragments of DNA digested with *Not* I (920 kb) and *Bss*HII (640 kb), indicating that the large genomic fragments recognized by this probe are altered by the *Ph* mutation (Fig. 3*A*). Based on the PFGE map, we estimate that *D5Buc2* maps 50 kb proximal to the *Ph* deletion (Fig. 1*A*).

Similarly, we were interested in identifying the position of the distal breakpoint of the *Rw* inversion. High molecular weight DNA isolated from C57BL/6J, C3H/HeJ, and *Rw*/C57BL/6J DNA was analyzed by PFGE using *Kit* and *Pdgfra* probes (Fig. 3 *B* and *C*). The *Kit* cDNA probe detected an altered fragment in *Mlu* I-digested *Rw*/C57BL/6J DNA. The *Pdgfra* cDNA clone detected altered DNA fragments in *Mlu* I-, *Bss*HII-, and *Not* I-digested *Rw*/C57BL/6J DNA. Since the *Mlu* I bands shared by *Kit* and *Pdgfra* are altered differently in *Rw* DNA, we have further confirmation that the *Rw*/C57BL/6J inversion breakpoint maps between *Kit* and *Pdgfra* (Fig. 1; Fig. 3 *B* and *C*). The FISH mapping of a *Pdgfra* YAC (8127) to *Rw*/C57BL/6J metaphase spreads suggests that sequences contained within the YAC, covering ≈450 kb, map within the *Rw* inversion (Fig. 2). Based on these data, the *Rw* breakpoint can be placed to the chromosomal segment between the distal YAC end clone, *D5Buc3*, and *Kit*.

DISCUSSION

We have established a high-resolution physical map of the region surrounding three members of the class III subfamily of RTKs (*Kit*, *Pdgfra*, and *Flk1*) (Fig. 1). This map indicates the position and extent of chromosomal rearrangements associated with the *Rw*, *Ph*, and W^{19H} mutations, which have profound developmental defects ranging from mild pigmentation anomalies in heterozygotes to embryonic lethality in homozygous mice.

The long-range restriction map spans 2.8 Mb and indicates the position of the *Kit*, *Pdgfra*, and *Flk1* genes and an anonymous mouse brain cDNA clone, *D5Mnl25*. The close genetic linkage between the *Flk1* and the *Kit*/*Pdgfra* cluster

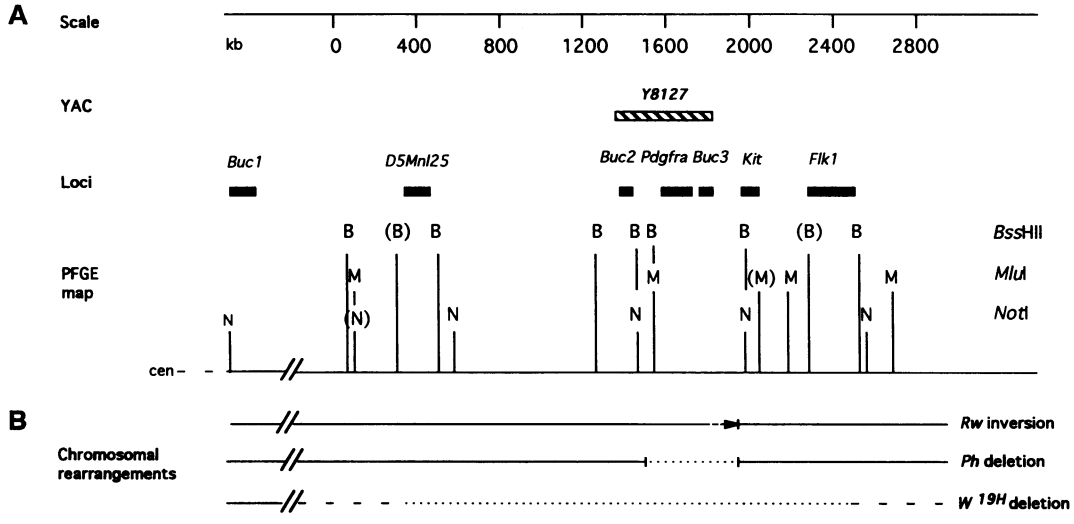

FIG. 1. Physical map of the *W–Ph–Rw* chromosomal region. (*A*) Long-range restriction map of C57BL/6J DNA constructed with the data in Table 1. Map indicates sites for the enzymes *Not* I (N), *Mlu* I (M), and *Bss*HII (B). Partially cut sites are shown in parentheses. Scale (kb) is shown above the map. Positions of probes are indicated by solid rectangles above the map (longer solid boxes indicate the limits of uncertainty of probe locations). *D5Buc1*, *D5Buc2*, and *D5Buc3* loci are indicated as *Buc1*, *Buc2*, and *Buc3*. Hatched box indicates position of the YAC clone Y8127. (*B*) Chromosomal rearrangements associated with *Ph*, W^{19H}, and *Rw* chromosomes determined in this study and in previously published reports, including the deletion of *Pdgfra* in the *Ph* mutation (12–15); deletion of *Kit*, *D5Mnl25*, and *Pdgfra* in W^{19H} (5, 6, 14, 15, 17); and inversion of the *D5Buc1* to *En2* region on the *Rw* chromosome (21). In this study, the extent of the *Ph* and W^{19H} chromosomal abnormalities was determined by a combination of deletion mapping and PFGE analysis. Dotted lines indicate deleted segments; dashed lines indicate limits of uncertainty of breakpoint locations. Position of the distal breakpoint of the *Rw* inversion (arrow) was determined by FISH mapping and PFGE analysis, as illustrated in Figs. 2 and 3. Position of *D5Buc1* on the physical map is inferred from genetic data (21), deletion mapping, and hybridization of *D5Buc1* and *D5Mnl25* to a *Not* I fragment of the same size (≈3500 kb).

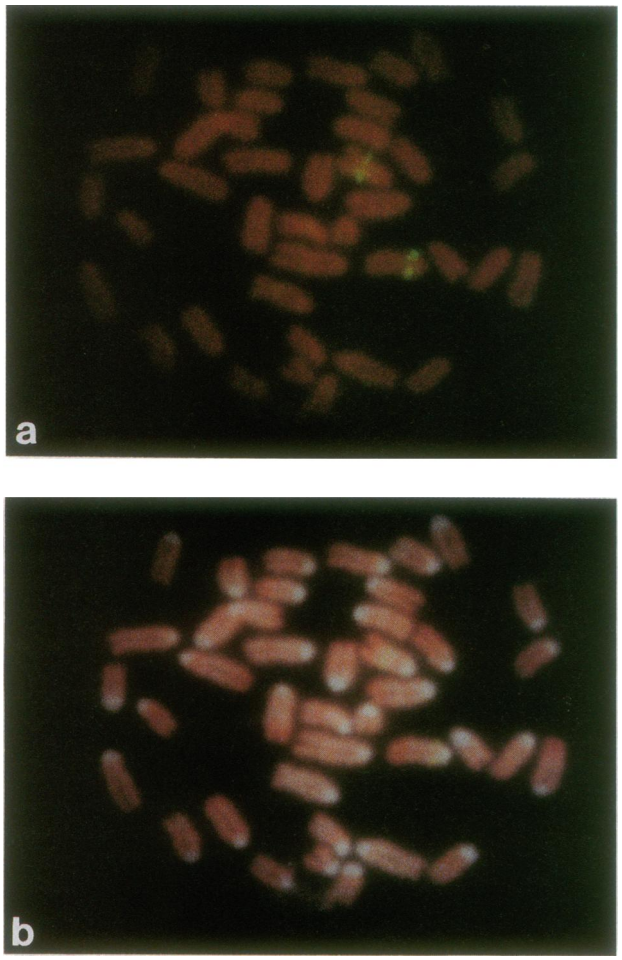

FIG. 2. FISH of the *Pdgfra*-containing YAC to *Rw*/+ metaphase spreads. (*a*) PI-counterstained spreads showing biotin-labeled probe (avidin–FITC detection). (*b*) DAPI-PI banded chromosomes are shown.

reported by Matthews *et al.* (24) is verified by placing the *Flk1* locus on the physical map 300–500 kb distal to *Kit*. The analysis of *Flk1* in *Ph*, *Rw*, and W^{19H} DNA revealed that this locus maps outside the *Ph* deletion, 500–700 kb distal to the breakpoint of the *Rw* inversion, but within the W^{19H} deletion. The W^{19H} deletion has been previously estimated to encompass 2–7 cM (16) and the presented physical map covers ≈2 Mb of that region located proximal to *Kit* and *Pdgfra*. The relative order of loci along the chromosome, with *D5Buc1* being the most proximal locus and *Flk1* the most distal, was determined by FISH analysis of the *Rw* inversion. The data generated by deletion mapping combined with the genetic data (21) place the proximal breakpoint of W^{19H} between *D5Buc1* and *D5Mnl25* and the position of the distal breakpoint between *Flk1* (the most distal locus on our map as shown in Fig. 1) and α-casein (*Csna*), a locus that has been mapped distal to the W^{19H} deletion (17).

The limits of the *Ph* deletion have been defined from our long-range restriction map: the deletion is not less than 45 kb and not more than 550 kb and includes the entire *Pdgfra* gene. The proximal breakpoint of the *Ph* deletion maps between *D5Buc2* and *Pdgfra*, while the distal breakpoint maps between *D5Buc3* and *Kit*. Although it is not clear from the data presented in this study whether *Pdgfra* is the only gene disrupted by the deletion, the map defines the limits of the region that should be searched for the presence of other affected genes. Furthermore, the distal breakpoint of the *Rw* inversion has been placed in the intergenic region between *Kit* and *Pdgfra*.

Comparison of the physical mapping data of the *Ph–W–Rw* chromosomal region (Fig. 4) and the results of complementation analysis involving the *Rw*, *Ph*, and W^{19H} mutations suggest that the lethality of these mutations may have a different basis (1, 16). All three mutations, W^{19H}, *Ph*, and *Rw*, are associated with embryonic lethality in homozygotes. W^{19H}/W^{19H} embryos die around implantation (16), *Ph/Ph* embryos usually die between the 9th and 12th days (11), whereas *Rw/Rw* embryos die probably around the 9.5th day of gestation (ref. 11; C. Lo, D.L.N., and M.B., unpublished data). The evidence that the recessive lethality of the *Rw* mutation is due to a mutation in a gene distinct from the loci affected by *Ph* and *W* comes from complementation studies with W^{19H}. *Rw* +/+ W^{19H} animals are viable, fertile, and depigmented except for the head area (ref. 16; M. Lyon, personal communication). The viability of *Rw* +/+ W^{19H} mice indicates that the gene whose disruption is responsible for the lethality of *Rw/Rw* embryos cannot be located within the W^{19H} deletion—i.e., at the distal breakpoint of the *Rw* inversion. In contrast, *Ph* +/+ W^{19H} heterozygotes are not viable, suggesting that the recessive lethality of *Ph* maps within the W^{19H} deletion (16). Therefore, if we assume that the mutant phenotype of *Rw/Rw* embryos is due to the inversion, it is very likely that the lethality associated with the *Rw* mutation is due to disruption of a gene located on the proximal breakpoint of the *Rw* inversion. However, it is possible that the lethality is the result of an inversion-independent mutation on the same chromosome, as in another irradiation-induced mutation, bare patches (*Bpa*) on mouse chromosome X (34). If this is the case, our physical map places the *Rw/Rw* lethality factor at least 1.6 Mb proximal to *Kit* and *Pdgfra* (outside the W^{19H} deletion).

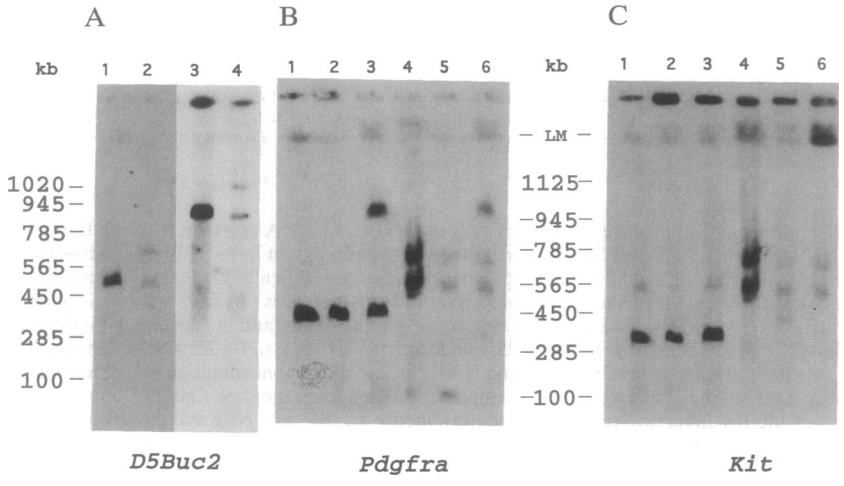

FIG. 3. PFGE analysis of chromosomal rearrangements associated with the *Rw* and *Ph* mutations. (*A*) PFGE analysis of the YAC end clone *D5Buc2* hybridized to C57BL/6J (lane 1) and *Ph*/C57BL/6J (lane 2) DNA digested with *Bss*HII; C57BL/6J (lane 3) and *Ph*/C57BL/6J (lane 4) DNA digested with *Not* I. (*B*) PFGE analysis of *Pdgfra* hybridized to C57BL/6J (lane 1), C3H/He (lane 2), and *Rw*/C57BL/6J (lane 3) DNA digested with *Bss*HII; C57BL/6J (lane 4), C3H/He (lane 5), and *Rw*/C57BL/6J (lane 6) digested with *Mlu* I. (*C*) PFGE analysis of *Kit* hybridized to C57BL/6J (lane 1), C3H/He (lane 2), and *Rw*/C57BL/6J (lane 3) DNA digested with *Bss*HII; C57BL/6J (lane 4), C3H/He (lane 5), and *Rw*/C57BL/6J (lane 6) digested with *Mlu* I. High molecular weight DNA was prepared from spleens. Electrophoresis was carried out for 28 hr in a 1% agarose gel in an electric field gradient of 6 V/cm at 14°C with a pulse time of 12.55 sec on a CHEF mapper PFGE apparatus (Bio-Rad).

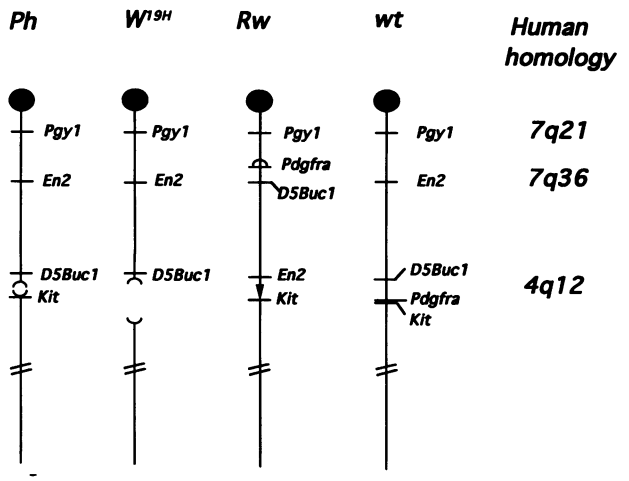

FIG. 4. Summary of analysis of chromosomal organization of the *W–Ph–Rw* region on wild-type and mutant chromosomes. Deduced map positions of chromosome 5 loci on the wild-type chromosome (*wt*) and the mutant chromosomes *Ph*, W^{19H}, and *Rw* based on data presented in this study and by others (5, 6, 14, 15, 17, 21). Brackets indicate approximate positions of the breakpoints; however, the extent of the deletions is not accurately represented. Arrow indicates position of the distal breakpoint of the *Rw* inversion. Positions of homologous segments in the human genome (33) are indicated on the right.

Rw +/+ *Ph* double heterozygotes are viable although the pigmentation defect in these double mutants is more pronounced than either mutation alone (1). This observation offers further support for the conclusion that the recessive lethalities of *Rw* and *Ph* are due to mutations in different genes. However, it does not exclude the possibility that the dominant coat color defect in *Ph* and *Rw* is due to the disruption of *Kit* or *Pdgfra* regulatory sequences. Recent observations by Duttlinger *et al.* (10) indicate that the W^{sh} mutation, which is associated with a pigmentation defect but lacks other pleiotropic defects (macrocytic anemia and sterility) present in the majority of *W* alleles, is probably a deletion that removes control elements associated with the *Kit* gene. Based on our data, these same regulatory elements could be disrupted by both the distal breakpoint of the *Ph* deletion and the distal breakpoint of the *Rw* inversion.

Since it is known that at least two homologous human RTK genes (*KIT* and *PDGFRA*) are closely linked on human chromosome 4 and that their deletion is associated with a comparable pigmentation defect in humans (18–20), the structural analysis of the *W–Ph–Rw* region will serve as a useful guide in comparative mapping efforts (Fig. 4). In addition, the proximal breakpoint of the *Rw* inversion is located in the segment of synteny conservation between mouse chromosome 5 and human chromosome 7 (33). Therefore, if the *Rw* lethality factor proves to be located at the proximal breakpoint of the *Rw* inversion, we predict the existence of a developmentally important gene causing late embryonic lethality in the homologous region on human chromosome 7 (q21 or q36).

We thank D. Solter in whose laboratory these studies were initiated; B. Cattanach for *Rw* mice; A. Bernstein, M. Mercola, I. Lemischka, and M. MacDonald for molecular probes; L. Stubbs, Z. Larin, and H. Lehrach for a *Pdgfra*-containing YAC clone; students who over the years contributed to this project; D. Stephenson, V. Chapman, S. Poethig, and P. Nolan for helpful discussions and comments on the manuscript; M. F. Lyon for communicating unpublished observations. These studies were supported by National Institutes of Health Grant HD 28410 (to M.B.), a Fellowship in IV Drug Abuse Research Center T32-DA07241 (to D.L.N.), a Predoctoral Fellowship from the National Institutes of Health Cellular and Molecular Biology Training Grant (GM07229-19) (to R.B.H.), and National Science Foundation Grant MCB 9210351 (to P.M.-D.).

1. Searle, A. G. & Truslove, G. M. (1970) *Genet. Res.* **15**, 227–235.
2. Reith, A. D. & Bernstein, A. (1991) in *Genome Analysis: Genes and Phenotypes*, eds. Davis, K. E. & Tilghman, S. M. (Cold Spring Harbor Lab. Press, Plainview, NY), Vol. 3, pp. 105–133.
3. Pawson, T. & Bernstein, A. (1990) *Trends Genet.* **6**, 350–356.
4. Silvers, W. K. (1979) *The Coat Colors of Mice* (Springer, New York), pp. 206–241.
5. Chabot, B., Stephenson, D. A., Chapman, V. M., Besmer, P. & Bernstein, A. (1988) *Nature (London)* **335**, 88–89.
6. Geissler, E. N., Ryan, M. A. & Housman, D. E. (1988) *Cell* **55**, 185–192.
7. Tan, J. C., Nocka, K., Ray, P., Traktman, P. & Besmer, P. (1990) *Science* **247**, 209–212.
8. Nocka, K., Majumder, S., Chabot, B., Ray, P., Cervone, M., Bernstein, A. & Besmer, P. (1989) *Genes Dev.* **3**, 816–826.
9. Reith, A. D., Rottapel, R., Giddens, E., Brady, C., Forrester, L. & Bernstein, A. (1990) *Genes Dev.* **4**, 390–400.
10. Duttlinger, R., Manova, K., Chu, T. Y., Gyssler, C., Zelenetz, A. D., Bachvarova, R. F. & Besmer, P. (1993) *Development* **118**, 705–717.
11. Grüneberg, H. & Truslove, G. M. (1960) *Genet. Res.* **1**, 69–90.
12. Orr-Urtreger, A., Bedford, M. T., Do, M.-S., Eisenbach, L. & Lonai, P. (1992) *Development* **115**, 289–303.
13. Schatteman, G. C., Morrison-Graham, K., Van Koppen, A., Weston, J. A. & Bowen-Pope, D. F. (1992) *Development* **115**, 123–131.
14. Stephenson, D. A., Mercola, M., Anderson, E., Wang, C., Stiles, C. D., Bowen-Pope, D. F. & Chapman, V. M. (1991) *Proc. Natl. Acad. Sci. USA* **88**, 6–10.
15. Smith, E. A., Seldin, M. F., Martinez, L., Watson, M. L., Choudhury, G. G., Lalley, P. A., Pierce, J., Aaronson, S., Barker, J., Naylor, S. L. & Sakaguchi, A. Y. (1991) *Proc. Natl. Acad. Sci. USA* **88**, 4811–4815.
16. Lyon, M. F., Glenister, P. H., Loutit, J. F., Evans, E. P. & Peters, J. (1984) *Genet. Res.* **44**, 161–168.
17. Geissler, E. N., Cheng, S. V., Gusella, J. F. & Housman, D. E. (1988) *Proc. Natl. Acad. Sci. USA* **85**, 9635–9639.
18. Fleischman, R. A., Saltman, D. L., Stastny, V. & Zneimer, S. (1991) *Proc. Natl. Acad. Sci. USA* **88**, 10885–10889.
19. Spritz, R. A., Droetto, S. & Fukushima, Y. (1992) *Am. J. Med. Genet.* **44**, 492–495.
20. Fleischman, R. A. (1993) *Trends Genet.* **9**, 285–290.
21. Stephenson, D. A., Lee, K.-h., Nagle, D. L., Yen, C.-H., Morrow, A., Miller, D., Chapman, V. M. & Bucan, M. (1994) *Mamm. Genome*, in press.
22. Besmer, P., Murphy, J. E., George, P. C., Qiu, F., Bergold, P. J., Lederman, L., Snyder, H. W., Jr., Brodeur, D., Zuckerman, E. E. & Hardy, W. D. (1986) *Nature (London)* **320**, 415–421.
23. Matsui, T., Heidaran, M., Miki, T., Popescu, N., La Rochelle, W., Kraus, M., Pierce, J. & Aaronson, S. (1989) *Science* **243**, 800–804.
24. Matthews, W., Jordan, C. T., Gavin, M., Jenkins, N. A., Copeland, N. G. & Lemischka, I. R. (1991) *Proc. Natl. Acad. Sci. USA* **88**, 9026–9030.
25. Hsieh, C.-L., Navankasattusas, S., Escobedo, J. A., Williams, L. T. & Francke, U. (1991) *Cytogenet. Cell Genet.* **56**, 160–163.
26. Wang, C., Kelly, J., Bowen-Pope, D. F. & Stiles, C. D. (1990) *Mol. Cell. Biol.* **10**, 6781–6784.
27. Herrmann, B. G., Barlow, D. P. & Lehrach, H. (1987) *Cell* **48**, 813–825.
28. Herrmann, B. G., Bucan, M., Mains, P. E., Frischauf, A.-M., Silver, L. M. & Lehrach, H. (1986) *Cell* **44**, 469–476.
29. Larin, Z., Monaco, A. P. & Lehrach, H. (1991) *Proc. Natl. Acad. Sci. USA* **88**, 4123–4127.
30. Green, E. D. & Olson, M. V. (1990) *Proc. Natl. Acad. Sci. USA* **87**, 1213–1217.
31. Arveiler, B. & Porteous, D. J. (1991) *Technique* **3**, 24–28.
32. Sawyer, J. R., Moore, M. M. & Hozier, J. C. (1987) *Chromosoma* **95**, 350–358.
33. Nadeau, J. H., Davisson, M. T., Doolittle, D. P., Grant, P., Hillyard, A. L., Kosowsky, M. R. & Roderick, T. H. (1992) *Mamm. Genome* **3**, 480–536.
34. Evans, E. P. & Phillips, R. J. S. (1975) *Nature (London)* **256**, 40–41.